

Radial Basis Function Assisted Reduced Complexity In-phase/Quadrature-phase Turbo Equalisation of Coded Modulation Schemes

M. S. Yee, S. X. Ng and ¹L. Hanzo

Dept. of ECS, University of Southampton, SO17 1BJ, UK.

Tel: +44-23-8059 3125, Fax: +44-23-8059 4508

Email: ¹lh@ecs.soton.ac.uk, <http://www-mobile.ecs.soton.ac.uk>

Abstract – A Radial Basis Function (RBF) assisted reduced complexity In-phase/Quadrature-phase (I/Q) Turbo Equalisation (TEQ) scheme is investigated in the context of Trellis Coded Modulation (TCM), Turbo TCM (TTCM), Bit-Interleaved Coded Modulation (BICM) and iteratively decoded BICM (BICM-ID). The proposed schemes are characterised in performance terms, when communicating over frequency selective Rayleigh fading channels. The RBF-I/Q-TEQ-TTCM achieved a similar performance to the full-complexity RBF-TEQ-TTCM, while attaining a complexity reduction factor of 36 in terms of the required additions/subtractions and a factor 9 in terms of the multiplications/divisions necessitated.

1. INTRODUCTION

Spectral efficiency is of primary concern in mobile communication systems owing to the scarcity and high price of the radio spectrum available for mobile radio services. In an effort to efficiently exploit the available spectrum, Coded Modulation (CM) schemes, which are based on combining the functions of channel coding and modulation, were proposed [1]. In this contribution, Trellis Coded Modulation (TCM) [1], Turbo TCM (TTCM) [1], Bit-Interleaved Coded Modulation (BICM) [1] and iteratively decoded BICM (BICM-ID) [1] will be studied. Furthermore, channel equalisation is invoked for mitigating the effects of Inter Symbol Interference (ISI) in the context of single carrier modulation, when communicating over frequency selective channels.

A Radial Basis Function (RBF) based equaliser (RBF-EQ) [2] constitutes a non-linear equalisation scheme, which formulates the channel equalisation procedure as a classification problem. The application of non-linear RBF based equalisers has been studied in conjunction with channel codecs [2], space-time codecs [3] as well as turbo-equalisers (TEQ) [2, 4]. The Bit Error Ratio (BER) performance of RBF-based turbo equalisation (RBF-TEQ) was presented in [2, 4] in the context of Quadrature Amplitude Modulation (QAM), which was found similar to that of the conventional trellis-based turbo equaliser (CT-TEQ) [5]. The RBF-assisted schemes are however capable of maintaining a lower complexity than their conventional trellis-based counterparts, when communicating over both dispersive Gaussian and Rayleigh faded channels, while maintaining a similar performance. The complexity of the RBF-TEQ scheme can be further reduced by invoking the In-phase/Quadrature-phase (I/Q) turbo equalisation (I/Q-TEQ) technique [2], while maintaining a similar perfor-

mance to that of the CT-TEQ. Recently, RBF-TEQ was studied in conjunction with coded modulation (RBF-TEQ-CM) in [6], where it was shown that performance gains can be achieved without bandwidth expansion in the context of RBF-TEQ with the advent of using CM.

Motivated by these trends, in this contribution, we aim for further reducing the complexity of the RBF-TEQ-CM scheme with the employment of the I/Q-TEQ principle by introducing a novel RBF-I/Q-TEQ-CM scheme.

2. PRINCIPLE OF I/Q EQUALISATION

We denote the modulated signal by $s(t)$, which is transmitted over the dispersive channel characterised by the Channel Impulse Response (CIR) $h(t)$. The signal is also contaminated by the zero-mean Additive White Gaussian Noise (AWGN) $n(t)$ exhibiting a variance of $\sigma^2 = N_0/2$, where N_0 is the single-sided noise power spectral density. The received signal $r(t)$ is then formulated as [2]:

$$\begin{aligned} r(t) &= s(t) * h(t) + n(t) \\ &= [s_I(t) + js_Q(t)] * [h_I(t) + jh_Q(t)] \\ &+ n_I(t) + jn_Q(t) \\ &= r_I(t) + jr_Q(t), \end{aligned} \quad (1)$$

where we have:

$$\begin{aligned} r_I(t) &= s_I(t) * h_I(t) - s_Q(t) * h_Q(t) + n_I(t) \\ r_Q(t) &= s_I(t) * h_Q(t) + s_Q(t) * h_I(t) + n_Q(t), \end{aligned} \quad (2)$$

since the CIR $h(t)$ is complex-valued and therefore consists of the I component $h_I(t)$ and Q component $h_Q(t)$. On the same note, $s_I(t)$ and $s_Q(t)$ are the I and Q components of $s(t)$, while $n_I(t)$ and $n_Q(t)$ denote the corresponding AWGN components. Both of the received I/Q signals, namely $r_I(t)$ and $r_Q(t)$ of Equation 2 become dependent on both $s_I(t)$ and $s_Q(t)$ owing to the cross-coupling effect imposed by the channel having a complex CIR. Hence a conventional channel equaliser, regardless of whether it is an iterative or non-iterative equaliser, would have to consider the effects of this cross-coupling.

However, it was shown in [2] that we can compute the I and Q components of the decoupled channel output $r'(t)$, as though they were dependent on $s_I(t)$ or $s_Q(t)$ only, in the context of the following

equations [2]:

$$\begin{aligned}
r'_I(t) &= s_I(t) * h(t) + n_I(t) \\
&= s_I(t) * h_I(t) + j[s_I(t) * h_Q(t)] + n(t) \\
r'_Q(t) &= -s_Q(t) * h(t) + n_Q(t) \\
&= -(s_Q(t) * h_I(t) + j[s_Q(t) * h_Q(t)]) + n(t).
\end{aligned} \tag{3}$$

More explicitly, the removal of the cross-coupling imposed by the complex CIR is facilitated by generating the estimates $\hat{s}_I(t)$ and $\hat{s}_Q(t)$ of the transmitted signal [7] with the aid of the reliability information generated by the channel decoder and then by cancelling the cross-coupling effects imposed by the channel, yielding $r'_I(t)$ and $r'_Q(t)$, respectively. Consequently, we can equalise $s_I(t)$ and $s_Q(t)$ independently, hence reducing the number of channel states and the associated complexity quite significantly.

3. RBF ASSISTED TURBO EQUALISATION

The RBF network based equaliser is capable of utilising the *a priori* information provided by the channel decoder and in turn provide the decoder with the *a posteriori* information concerning the coded bits [4]. We will now provide a brief description of the symbol-based coded modulation assisted RBF aided turbo equalisation philosophy.

The conditional probability density function (PDF) of the i th symbol, $i = 1, \dots, \mathcal{M}$, associated with the i th subnet of the \mathcal{M} -ary RBF channel equaliser having a feedforward order of m is given by [2]:

$$f_{RBF}^i(\mathbf{r}(t)) = \sum_{j=1}^{n_{s,i}} w_j^i \varphi(|\mathbf{r}(t) - \mathbf{c}_j^i|), \tag{4}$$

$$w_j^i = p_j^i (2\pi\sigma_\eta^2)^{-m/2}, \tag{5}$$

$$\begin{aligned}
\varphi(x) &= \exp\left(\frac{-x^2}{2\sigma_\eta^2}\right) \\
i &= 1, \dots, \mathcal{M}, \quad j = 1, \dots, n_{s,i}
\end{aligned} \tag{6}$$

where \mathbf{c}_j^i , w_j^i and $\varphi(\cdot)$ are the RBF's centres, weights and activation function, respectively, and σ_η^2 is the noise variance of the channel.

The term

$\mathbf{r}(t) = [r(t) \ r(t-1) \ \dots \ r(t-m+1)]^T$ is the m -dimensional channel output vector stored in the memory of the RBF equaliser. The RBF's centres \mathbf{c}_j^i are assigned to the channel output states \mathbf{r}_j^i . The channel output state, which is the product of the CIR matrix \mathbf{H} and the channel input state \mathbf{s}_j , is represented as follows [2]: $\mathbf{r}_j = \mathbf{H}\mathbf{s}_j$, where the z-transform of the CIR $h(t)$ having a memory of L symbols is represented by $H(z) = \sum_{n=0}^L h_n z^{-n}$ and \mathbf{H} is an $m \times (m+L)$ matrix given by the CIR taps as follows:

$$\mathbf{H} = \begin{bmatrix} h_0 & h_1 & \dots & h_L & \dots & 0 \\ 0 & h_0 & \dots & h_{L-1} & \dots & 0 \\ \vdots & \vdots & & & & \vdots \\ 0 & 0 & h_0 & \dots & h_{L-1} & h_L \end{bmatrix}. \tag{7}$$

The channel input state \mathbf{s}_j is given by the j th combination of the $(L+m)$ number of possible transmitted symbols, namely by

$\mathbf{s}_j = [s_j(t) \ \dots \ s_j(t-1) \ \dots \ s_j(t-L-m+1)]^T$. The

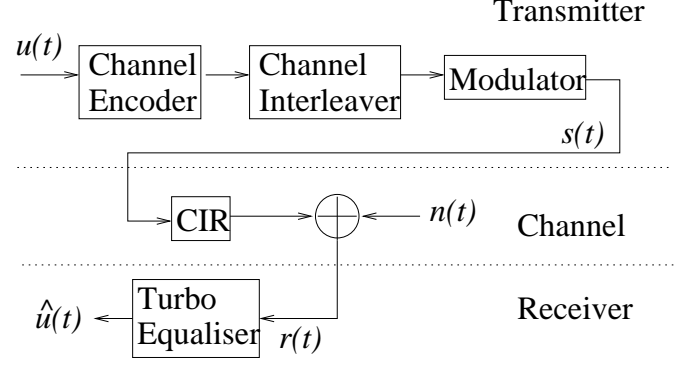


Figure 1: A coded \mathcal{M} -QAM system employing a turbo equaliser at the receiver.

term p_j^i in Equation 5 is the probability of occurrence of the channel state \mathbf{r}_j^i and it determines the values of the RBF weights w_j^i . The actual number of channel states $n_{s,i}$ is determined by the specific design of the algorithm used for reducing the number of channel states from the optimum number of \mathcal{M}^{m+L-1} [2] to an implementationally more affordable value. The probability of the channel states \mathbf{r}_j^i and therefore the weights of the RBF equaliser can be derived from the probability values of the transmitted symbols/bits, as estimated by the channel decoder.

In the RBF-I/Q-EQ scheme, we utilised the principle of separate I/Q equalisation [2], as outlined in Section 2, where two separate RBF equalisers were used for the in-phase and quadrature component of the transmitted symbols. The in-phase-RBF-EQ has RBF centres, which consist of the in-phase decoupled channel output $r'_I(t)$ of Equation 2 and vice-versa for the quadrature-RBF-EQ. The number of possible channel output states is reduced, since the decoupled channel output $r'(t)$ is dependent on $\sqrt{\mathcal{M}}$ number of possible in-phase or quadrature-phase transmitted symbols instead of the original \mathcal{M} symbols. The following section describes, how the RBF-I/Q-EQ is incorporated into the schematic of the turbo equaliser.

4. SYSTEM OVERVIEW

The schematic of the coded \mathcal{M} -QAM system employing a TEQ at the receiver is shown in Figure 1. The transmitted $(m-1)$ -bit information symbols are encoded by the rate- $(m-1)/m$ CM encoder, interleaved and mapped to an \mathcal{M} -ary modulated symbol where we have $\mathcal{M} = 2^m$. We utilised 16-level QAM (16QAM) for attaining an effective transmission throughput of $m-1 = 3$ information Bits Per Symbol (BPS). The 16QAM-based CM schemes employed exhibited a similar decoding complexity for the sake of a fair comparison. More specifically, a component TCM (BICM) code memory of 3 was used for the TTCM (BICM-ID) scheme. The number of iterations used by the TTCM (BICM-ID) scheme was fixed to 4 (8) and hence the iterative scheme exhibited a similar decoding complexity to the non-iterative TCM (BICM) scheme of memory 6, when expressed in terms of the number of coding states [1].

Figure 2 illustrates the schematic of the turbo equaliser utilising two reduced-complexity RBF-I/Q equalisers. We expressed the non-binary Logarithmic Probability (LP) of the \mathcal{M} -ary symbols processed

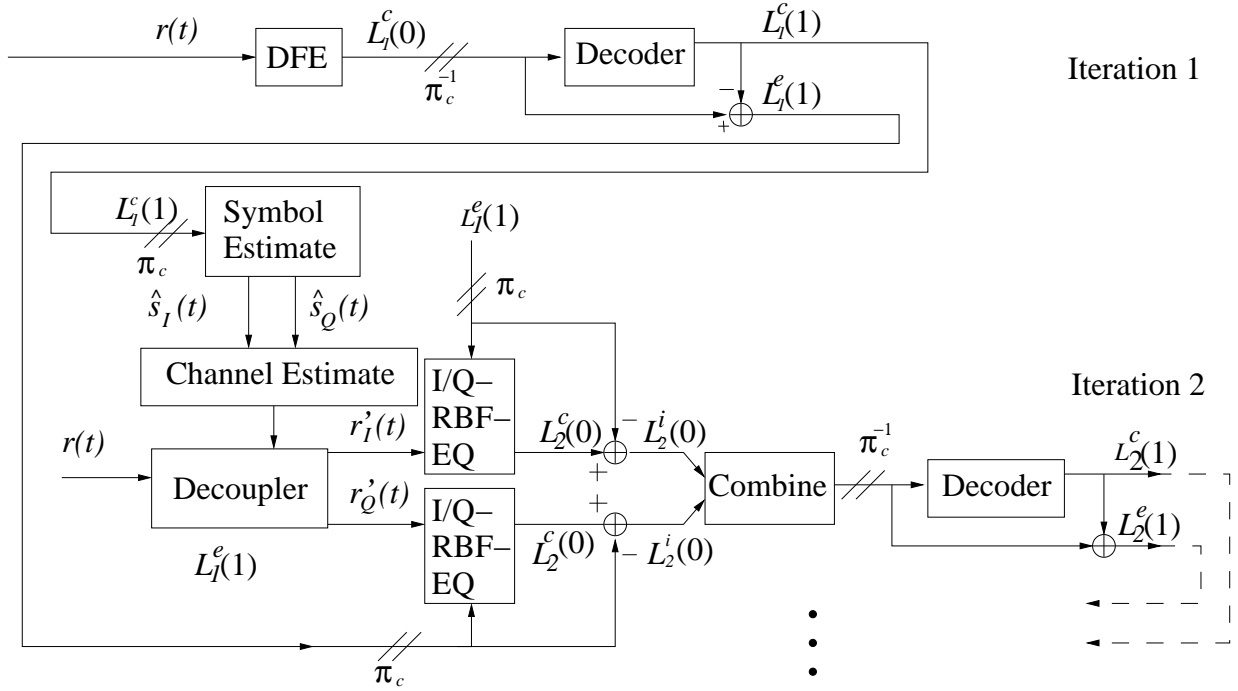


Figure 2: Schematic of the turbo equaliser employing a DFE and a SISO channel decoder in the first turbo equalisation iteration. In subsequent iterations, two RBF-I/Q-EQs and one SISO channel decoder are employed. The notation π_c represents a channel interleaver, while π_c^{-1} is used to denote a channel deinterleaver.

by of the equaliser or decoder using vector notations, according to the approach of [8], but using different specific notations. Explicitly, the superscript used in Figure 2 denotes the nature of the LP, namely ‘c’ is used for the composite a *posteriori* information [9], ‘i’ for the combined channel and extrinsic information [9] and ‘e’ for the extrinsic information [9]. By contrast, The subscripts in Figure 2 are used for representing the iteration index, while the argument within the round brackets () indicates the index of the receiver stage, where the equalisers are denoted as receiver stage 0, while the channel decoder as receiver stage 1.

The conventional minimum mean square error DFE seen at the top left corner of Figure 2 is used during the first turbo equalisation iteration for providing soft decisions in the form of the LP $L_1^p(0)$ for the CM decoder. Invoking the DFE during the first iteration constitutes a low-complexity approach to providing an initial estimate of the transmitted symbols, as compared to the more complex RBF-I/Q-EQ. The symbol-based MAP channel decoder [1] of Figure 2 generates the a posteriori LP $L_1^p(1)$ and from that, the extrinsic information of the encoded symbols $L_1^e(1)$ is extracted. In the next iteration, the a posteriori LP $L_1^p(1)$ is used for regenerating estimates of the I and Q components of the transmitted signal, namely $\hat{s}_I(t)$ and $\hat{s}_Q(t)$, as seen in the ‘Symbol Estimate’ block of Figure 2. The a posteriori information was transformed from the logarithmic domain to modulated symbols using the approach employed in [7]. The estimated transmitted quadrature components $\hat{s}_I(t)$ and $\hat{s}_Q(t)$ are then convolved with the estimate of the CIR $h(t)$. The CIR can be estimated using a variety of techniques based on the training sequence of the transmission burst seen in Figure 3, although we assumed perfect CIR estimation in this

contribution. At the decoupler block of Figure 2, the resultant signal is used for removing the I/Q cross-coupling effect, as seen in Equation 2, according to Equation 3 from both quadrature components of the transmitted signal, yielding $r'_I(t)$ and $r'_Q(t)$ of Equation 3.

After the decoupling operation, $r'_I(t)$ and $r'_Q(t)$ are passed to the RBF-I/Q-EQ in the schematic of Figure 2. In addition to these received quadrature signals, the RBF-I/Q-EQ also processes the a priori information received, which is constituted by the extrinsic LPs $L_1^e(1)$ derived from the previous iteration, and generates the a posteriori information $L_2^p(0)$. Subsequently, the combined channel and extrinsic information $L_2^i(0)$ is extracted from both RBF-I/Q-EQs in Figure 2 and combined, before being passed to the Log-MAP channel decoder. As in the first turbo equalisation iteration, the a posteriori and extrinsic information of the encoded symbol, namely $L_2^p(1)$ and $L_2^e(1)$, respectively, are evaluated. Subsequent turbo equalisation iterations obey the same sequence of operations, until the iteration termination criterion is met.

5. RESULTS AND DISCUSSION

We employed the Jacobian RBF-DFE of [2, 10], which reduced the complexity of the RBF equaliser by utilising the Jacobian logarithmic function [2] and decision feedback assisted RBF-centre selection [2] as well as a TEQ scheme using a symbol-based MAP channel decoder [1]. The RBF-DFE based TEQ is specified by the equaliser’s decision delay τ , the feedforward order m and the feedback order n . The number of RBF nodes is $n_{s,i} = \mathcal{M}^{L+m-n}$ and the number of scalar channel states of the Jacobian RBF equaliser is $n_{s,f} = \mathcal{M}^{L+1}$,

where we have $\bar{\mathcal{M}}=\mathcal{M}$ for the non-I/Q based full-complexity RBF-TEQ system, while $\bar{\mathcal{M}}=\sqrt{\mathcal{M}}$ for the I/Q based reduced-complexity RBF-TEQ system. The computational complexity associated with generating the *a posteriori* LP for the Jacobian RBF equaliser is given by [10]: $n_{s,i}(m+2) - 2\bar{\mathcal{M}} + n_{s,f}$ number of additions/subtractions and $2n_{s,f}$ multiplications/divisions. Here, we employed $\tau=2$, $m=3$ and $n=1$ for the RBF-TEQ, as well as $m=7$ and $n=1$ for the conventional DFE. Therefore, the 'per-iteration' complexity of the full-RBF-TEQ expressed in terms of the number of additions/subtractions and multiplications/divisions is about 20704 and 512, respectively, while that of the RBF-I/Q-TEQ is about 328 and 32, respectively.

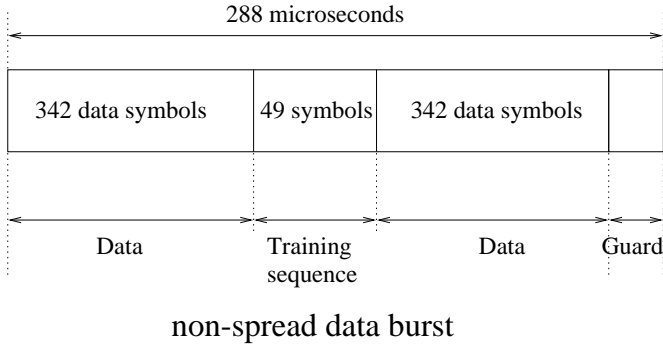


Figure 3: Transmission burst structure of the FMA1 non-spread speech burst of the FRAMES proposal [11].

The transmission burst structure used in this system is the FMA1 non-spread data burst specified by the Pan-European FRAMES proposal [11], which is shown in Figure 3. When considering a Time Division Multiple Access (TDMA) system of 16 slots per 4.615ms TDMA frame, the transmission burst length is 288 μ s, as shown in Figure 3. In our investigations, the transmission delay was limited to approximately $8 \times 4.615ms = 37ms$. This corresponds to a transmission delay of 8 TDMA frames and a channel interleaver depth of $8 \times 684 = 5472$ symbols can be employed. A two-path, symbol-spaced CIR of equal tap weights was used, which can be expressed as $h(t) = 0.707 + 0.707z^{-1}$ where $L = 1$ and the Rayleigh fading statistics obeyed a normalised Doppler frequency of 3.25×10^{-5} . The fading magnitude and phase was kept constant for the duration of a transmission burst, a condition which we refer to as employing transmission burst-invariant fading.

The BER versus signal to noise ratio per bit, namely E_b/N_0 performance of the 16QAM-based RBF-I/Q-TEQ-TTCM, -TTCM, -BICM and -BICM-ID schemes is shown in Figure 4, where the performance of the CM schemes based on the conventional DFE used during the first iteration was significantly improved after another five TEQ iterations based on the RBF-DFE. Explicitly, the RBF-I/Q-TEQ-TTCM performance recorded after the sixth TEQ iteration is about 7.8 dB better than that after the first iteration employing the conventional DFE and it is only 2.2 dB away from the identical-throughput AWGN-based uncoded 8PSK scheme.

The coding gain of the various 16QAM-based RBF-I/Q-TEQ assisted CM schemes can be found by comparing their BER curves to that of the conventional DFE assisted uncoded-8PSK scheme, as shown in Figure 4 for an identical bandwidth/throughput scenario.

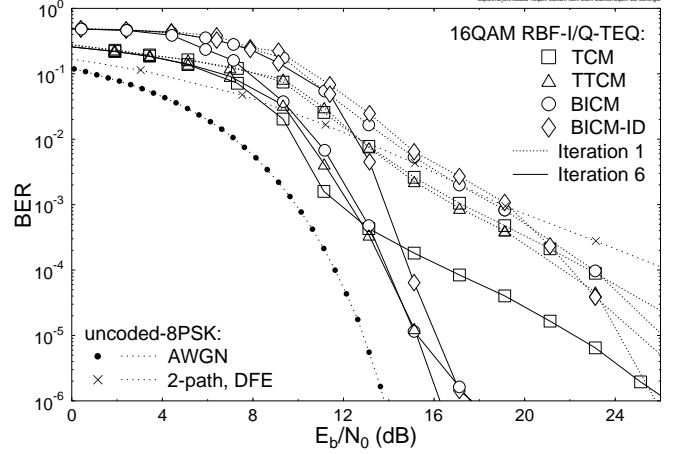


Figure 4: Performance of the 16QAM based RBF-I/Q-TEQ-TTCM, -TTCM, -BICM, -BICM-ID schemes when communicating over the two-path, equal tap-weight dispersive Rayleigh fading channel. The performance of the uncoded conventional 8PSK scheme communicating over the non-dispersive AWGN channel is also shown as a benchmarker.

Specifically, the first iteration of the 16QAM-based RBF-I/Q-TEQ-CM scheme employed a conventional DFE, rather than the RBF-DFE, hence its performance is identical to that of the conventional DFE assisted CM-16QAM schemes. As we notice from Figure 4, the achievable coding gain of the various RBF-I/Q-TEQ assisted CM-16QAM schemes at the sixth iteration is significantly higher than that of the conventional DFE assisted CM-16QAM schemes, albeit this is achieved at a higher complexity. However, the complexity of the RBF-I/Q-TEQ scheme is still lower than that of the conventional trellis-based TEQ [2, 4].

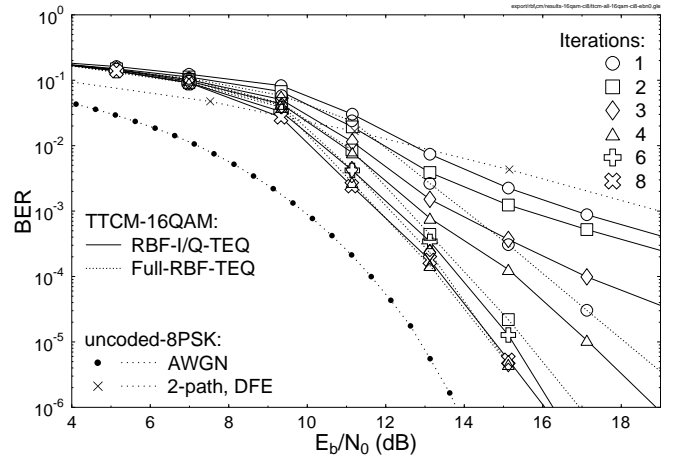


Figure 5: Performance of the 16QAM based RBF-I/Q-TEQ-TTCM and full-RBF-TEQ-TTCM schemes when communicating over the two-path, equal tap-weight dispersive Rayleigh fading channel. The performance of the uncoded conventional 8PSK scheme communicating over the non-dispersive AWGN channel is also shown as a benchmarker.

The performance of the 16QAM based RBF-I/Q-TEQ-TTCM scheme is compared to that of the full-RBF-TEQ-TTCM arrangement in Fig-

ure 5. We found that using more than eight and four TEQ iterations did not provide further significant gains for the RBF-I/Q-TEQ-TTCM and full-RBF-TEQ-TTCM schemes, respectively. The reduced complexity RBF-I/Q-TEQ-TTCM arrangement exhibits a worse performance during the first three iterations than that of the full-RBF-TEQ-TTCM scheme during the first iteration. This is due to the employment of a conventional DFE during the first iteration of the RBF-I/Q-TEQ-TTCM scheme, as well as owing to the imperfect I/Q decoupling effects, when unreliable symbol estimates are fed back to the input of the iterative scheme. However, more reliable symbol estimates become available with the aid of the iterative TEQ scheme during the forthcoming iterations and the performance of the RBF-I/Q-TEQ-TTCM scheme becomes comparable to that of the full-complexity RBF-TEQ-TTCM arrangement eventually. Explicitly, the performance of RBF-I/Q-TEQ-TTCM having eight iterations becomes similar to that of RBF-TEQ-TTCM having four iterations for BER values below 10^{-4} , as shown in Figure 5. Note that the complexity imposed by the conventional DFE during the first RBF-I/Q-TEQ iteration may be deemed insignificant compared to that of the remaining RBF based iterations. Hence, we should compare the complexity of the RBF-DFE assisted scheme using seven iterations in the context of the eight-iteration aided RBF-I/Q-TEQ-TTCM scheme characterised in Figure 5, to that of the four-iteration assisted full RBF-TEQ-TTCM scheme. Under these conditions, it can be shown that complexity reduction factors of $\frac{4}{7} \cdot \frac{20704}{328} \approx 36$ and $\frac{4}{7} \cdot \frac{512}{32} \approx 9$ were obtained in terms of the required number of additions/subtractions and multiplications/divisions, respectively.

6. CONCLUSION

In conclusion, the performance of the proposed RBF-I/Q-TEQ-CM scheme is significantly better than that of the conventional DFE assisted CM schemes, as evidenced in Figure 4. Our simulation results also show significant complexity reductions for the RBF-I/Q-TEQ-CM scheme, when compared to full-RBF-TEQ-CM arrangement, while achieving virtually the same performance. This is demonstrated in Figure 5 for TTCM scheme. Amongst the four CM schemes studied, the best performer is TTCM, followed by BICM, BICM-ID and TCM after the sixth iteration of the RBF-I/Q-TEQ arrangement, as evidenced by Figure 4 in terms of the BER attained.

7. ACKNOWLEDGEMENTS

The financial support of the European Union under the auspices of the SCOUT project, the EPSRC, Swindon UK and the Virtual Centre of Excellence (VCE) in Mobile Communications is gratefully acknowledged.

8. REFERENCES

- [1] L. Hanzo, T.H. Liew and B.L. Yeap, *Turbo Coding, Turbo Equalisation and Space Time Coding for Transmission over Wireless Channels*. New York, USA: John Wiley IEEE Press, 2002.
- [2] L. Hanzo, C. H. Wong, and M. S. Yee, *Adaptive Wireless Transceivers: Turbo-Coded, Turbo-Equalized and Space-Time Coded TDMA, CDMA and OFDM Systems*. John Wiley, IEEE Press, 2002.
- [3] M. S. Yee, B. L. Yeap, and L. Hanzo, "Turbo equalisation of convolutional coded space time trellis coded systems using radial basis function equalizers," in *Proceedings of Vehicular Technology Conference*, (Atlantic City, USA), Oct 7-11 2001.
- [4] M. S. Yee, B. L. Yeap, and L. Hanzo, "Radial basis function assisted turbo equalisation," in *Proceedings of IEEE Vehicular Technology Conference*, (Japan, Tokyo), pp. 640-644, IEEE, 15-18 May 2000.
- [5] G. Bauch, H. Khorram, and J. Hagenauer, "Iterative equalization and decoding in mobile communications systems," in *European Personal Mobile Communications Conference*, (Bonn, Germany), pp. 301-312, 30 September - 2 October 1997.
- [6] M. S. Yee, S. X. Ng and L. Hanzo, "Iterative radial basis function assisted turbo equalisation of various coded modulation schemes," *IEEE Vehicular Technology Conference*, pp. 1705-1709, May 2002.
- [7] A. Glavieux, C. Laot, and J. Labat, "Turbo equalization over a frequency selective channel," in *Proceedings of the International Symposium on Turbo Codes*, (Brest, France), pp. 96-102, 3-5 September 1997.
- [8] M. Gertsman and J. Lodge, "Symbol-by-symbol MAP demodulation of CPM and PSK signals on Rayleigh flat-fading channels," *IEEE Transactions on Communications*, vol. 45, pp. 788-799, July 1997.
- [9] L.R. Bahl and J. Cocke and F. Jelinek and J. Raviv, "Optimal Decoding of Linear Codes for Minimising Symbol Error Rate," *IEEE Transactions on Information Theory*, vol. 20, pp. 284-287, March 1974.
- [10] M. S. Yee, T. H. Liew and L. Hanzo, "Burst-by-Burst Adaptive Turbo-Coded Radial Basis Function-Assisted Decision Feedback Equalization," *IEEE Transactions on Communications*, vol. 49, pp. 1935-1945, November 2001.
- [11] A. Klein and R. Pirhonen and J. Skoeld and R. Suoranta, "FRAMES Multiple Access MODE 1 — Wideband TDMA with and without Spreading," in *Proceedings of the IEEE International Symposium on Personal, Indoor and Mobile Radio Communications (PIMRC)*, vol. 1, (Helsinki, Finland), pp. 37-41, 1-4 September 1997.